Investigation of Impact Damage on GFRP/MWCNT for Structural Health Monitoring

OZAN CAN ZEHNI, IAN KINLOCH, MARK BISSETT and CHRISTINA VALLES

ABSTRACT

The primary objective of the present study was to investigate the detection of Barely Visible Impact Damage (BVID) in composites, a crucial problem that needed to be addressed. To accomplish this, the researchers measured the resistance changes in two glass fibre layers coated with Multi-Walled Carbon Nanotubes (MWCNTs), embedded in the laminate, during the impact test. The results of the experiments performed at various impact energy levels indicated that resistance change could be effectively used to detect BVID. Furthermore, the maximum average resistance change ratio was found to be 9 % for 20J impact tests. The system's capability to detect repeated impact damage was further demonstrated through the execution of repeated impact tests. Additionally, the remaining strength values of the samples were determined by conducting compression tests after the impact tests. It was observed that the samples subjected to 20J impact damage experienced a loss of approximately 50 % in their strength. These findings emphasize the system's potential to predict the remaining strength of the material.

INTRODUCTION

Fibre-reinforced composites are widely employed in various fields, such as aerospace, automotive, and energy, due to their exceptional properties. The key factors driving their popularity are their high specific strength and stiffness, along with their ability to resist fatigue and corrosion, as well as their capacity for tailored mechanical properties [1]. However, the composites industry needs to overcome significant hurdles to address concerns related to structural affordability and safety. These challenges include reducing material and manufacturing expenses, ensuring consistent quality in manufacturing processes, developing effective joining techniques, mitigating damage during service, establishing reliable design guidelines, and enhancing maintenance and repair technologies for structural components [2]. Structural Health Monitoring (SHM) applications offer promising solutions to some of the challenges faced by the aviation industry [3]. SHM not only

Ozan Can Zehni, Cristina Valles, Mark Bissett, and Ian Kinloch, National Graphene Institute and School of Materials, University of Manchester, Manchester M13 9PL, UK. Email: ozan.zehni@postgrad.manchester.uk.ac

enhances flight safety but also optimizes maintenance time and costs by providing real-time data on structural damage, localization, and severity. Moreover, data obtained from SHM applications can be leveraged to develop design parameters for future aircraft.

Recent research has highlighted several SHM applications, such as vibration-based methods [4], acoustic emission-based methods [5], and methods based on changes in electrical properties [6][7], particularly for composite materials. Several SHM methods are adapted from Non-Destructive Testing (NDT) techniques, and most of them target Barely Visible Impact Damage (BVID) [8][9], a commonly observed form of damage, especially within the aviation industry, which results in an approximate 50 % reduction in the composite's strength [10]. Numerous studies and techniques have been documented in existing literature for detecting BVID, and one promising approach is the resistance change method, which relies on changes in electrical resistance to monitor strain, detect damage, determine its location, and identify its type. A significant advantage of this approach is that it does not require additional equipment or sensors, making it a cost-effective and practical solution for SHM.

Despite the abundance of literature on SHM applications for composites, their implementation on an industrial scale remains a challenge [11]. There are several reasons for this, including the anisotropic nature of composite structures, which gives rise to different types of damage mechanisms such as matrix cracks, fibre cracks, delamination, and debonding [12]. Moreover, environmental factors can impact the data obtained from composites during operation, making it difficult to achieve consistent results with SHM applications, unlike NDT methods.

This study aims to investigate the characteristics of BVID in glass fibre reinforced polymer (GFRP) and establish a simple and feasible SHM approach for detecting BVID and estimating the remaining strength of the material. Specifically, non-conductive glass fibres were coated with multi-walled carbon nanotubes (MWCNT), and impact tests were conducted at various energy levels using a drop tower. Unlike prior investigations in the field, this study utilizes the self-sensing properties of MWCNTs to measure the resistance change from two channels simultaneously during the impact test. This approach enables a comprehensive understanding of the impact damage in different layers in GFRP composites without sacrificing the mechanical properties of GFRP [13]. Subsequently, a compression after impact test (CAI) was performed on the damaged samples. The findings revealed a direct correlation between the level of applied impact energy and the resulting change in resistance. Furthermore, the permanent change in resistance demonstrated promising implications for the material's residual strength.

In the upcoming section, the experimental methodology will be thoroughly explained. Subsequently, the experimental results and their corresponding discussion will be presented. Finally, the study will conclude with the findings and implications drawn from the research.

EXPERIMENTAL METHODOLOGY

Materials and manufacturing

To prepare the coating solution, NC7000 (a type of thin multiwall carbon nanotubes produced by Nanocyl SA using the Catalytic Chemical Vapour Deposition process) was mixed with ethanol at a ratio of 1 ml per 0.2 mg of MWCNT. The mixture was sonicated for an hour to ensure proper dispersion of the

0.5%wt. MWCNTs in the ethanol. The spray coating method was then used to apply the MWCNT coating onto two woven glass fibres. As illustrated in Figure 1, the composite material is composed of 12 layers, with two MWCNT-coated layers situated above the bottom layer and below the top layer. Copper tape was used to attach cables to the MWCNT-coated glass fibres.

For this study, an E-glass fibre plain woven fabric (290g/m2, supplied by Easy Composites, UK) and a two-part low-viscosity infusion epoxy resin were chosen. The diglycidyl bisphenol-A epoxy resin (BiResin CR83, supplied by Sika Industry, Germany) and a hardener (Biresin CH83-10, supplied by Sika Industry, Germany) were mixed with a weight ratio of 1:0.3 and degassed for 45 minutes prior to vacuum-assisted resin infusion at ambient temperature. Once the laminates were completely infused with epoxy resin, they were placed in an oven to cure with the following cycle: 1 °C/min to 70 °C, then dwell for 12 hours at 70 °C, followed by natural cooling to ambient temperature.

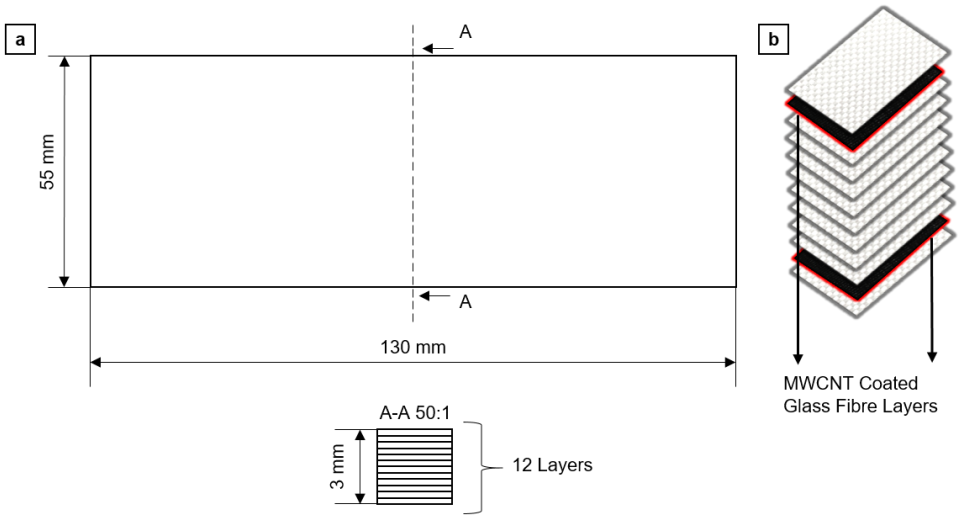

Figure 1. a) A schematically drawing of the impact test specimen. Drawing is not to scale, and all dimensions are in mm. b) The impact test specimen consists of 12 glass woven layers in total, with 2 MWCNT coated glass woven layers positioned below the top layer and above the bottom layer.

Impact Test and Electrical Measurement

The specimens were subjected to impact testing using an instrumented drop weight machine (Instron Ceast 9350) equipped with a 20 mm diameter hemispherical tup weighing 2.7 kg. The specimens were clamped between two plates, each with a circular opening (40 mm diameter), and the impact energy was varied by releasing the top from different heights. Four samples were tested for each of 5J, 12J, and 20J energy level respectively. Additionally, two samples were tested for multiple impact tests. To ensure the elimination of multiple impacts, the impact rig was equipped with a device. During the CAI, an anti-buckling guide was utilized to provide support to the specimen. A loading rate of 1 mm/min was employed during the compression tests.

The electrical resistance measurements were conducted using the National Instruments (NI) compact DAQ system specifically designed for this purpose. The NI 9264 (25 kS/s/ch Simultaneous, ±10 V, 16-Channel C Series Voltage Output Module) was connected to two channels for voltage output, and the current values

were subsequently measured using NI 9203 (200 kS/s, ±20 mA, 8-Channel C Series Current Input Module) at a frequency of 25 kHz for two channels. During the test, a continuous voltage was applied to the samples, and the changes in current were recorded. The ability of the samples to detect damage was assessed by determining the ratio of the change in resistance to the initial resistance, represented as $\Delta R/R_0$

EXPERIMENTAL RESULTS AND DISCUSSION

Variations in the initial resistance value are observed not only between different samples but also between the upper and lower channels of the same sample. This can be attributed to the random distribution of MWCNTs on the surface of the glass fibres, which creates diverse electrical pathways. To mitigate the impact of these initial value discrepancies, the ratio of resistance change to the initial resistance ($\Delta R/R_0$) is used in the calculations.

In Figure 2, the force and resistance change data of the samples under impact energies of 5J, 12J, and 20J are presented before, during, and after impact. As clearly demonstrated in the figure, there is a positive correlation between the impact response force and the measured $\Delta R/R_0$ for all applied energy levels. The duration of the impact test for all energy levels is approximately 3ms. During this time, the reaction force of the material increases and then begins to decrease, as indicated by the measured and calculated $\Delta R/R_0$ values in the experiment. Additionally, the upper and lower channel $\Delta R/R_0$ values exhibit variation due to the propagation of impact damage from top layer to the underlying layers. Notably, the $\Delta R/R_0$ value obtained from the lower channel during the impact test is higher for all energy levels, indicating significantly greater damage and reaction force in that region.

For the 5J impact energy, the resistance change in the upper channel was observed to be less than 1% during the impact test and returned to its initial value afterward. In contrast, the maximum $\Delta R/R_0$ in the lower layer was approximately 2 % during the experiment, with a permanent resistance less than 1 % after the test. This difference can be attributed to the reaction forces initiation from the first layer and its progression through the thickness, as explained earlier. During the impact test conducted with an energy level of 12J, it was observed that the maximum resistance change ratio in the upper layer exceeded 4 % during the test, with a permanent change of over 2 % after the test. In contrast to the 5J impact test, the 12J impact test caused a permanent resistance change of approximately 0.5 % in the upper layer. This indicates that the damage to the upper layer from the 12J impact resulted in a permanent resistance change parallel to the damaged area. In the case of the 20J impact test, the average maximum resistance value in the bottom layer was found to be approximately 9% during the test (see Figure 3b). As expected, the permanent resistance change was around 4 %, which is higher than the values obtained from the 5J and 12J tests (see Figure 3a). The results of the resistance change in the top layer revealed a maximum change of 4 % during the test, with a permanent change of 1.5 % thereafter (see Figure 3a).

Figure 4a depicts the impact test conducted five times with an energy level of 5J. Upon analysis of the resistance changes, it became evident that there is a correlation with the impact reaction force for each repetition. This demonstrates the ability to detect multiple impact damages that may occur during actual operation. Furthermore, it can be concluded that the resistance changes obtained for each repetition are nearly identical, and there is no increase in permanent damage for both channels. This is because the damage resulting from the 5J impact does not cause

any disruption in the MWCNTs' path. The change in resistance is primarily attributed to the elastic deformation caused by the reaction force during impact.

The results of impact tests with different energy levels (5J, 12J, and 20J) on a single sample are presented in Figure 4b. The resistance value of the sample increased proportionally with the reaction force generated by each impact energy level, indicating that the method can detect different impact damage levels that may occur in the same region during operation. Following the completion of the 5J impact test, the researchers proceeded to conduct the 12J impact test. The outcomes of this subsequent test revealed a permanent $\Delta R/R_0$ of approximately 2.5 % and a maximum $\Delta R/R_0$ of around 4 %, as measured during the experiment. Figure 3 depicts the average results, which clearly demonstrated a strong resemblance between the measurements obtained from samples solely exposed to the 12J impact and the anticipated results. This similarity can be attributed to the limited damage caused by the 5J impact energy level to the MWCNT path within the samples. However, in the case of the 20J impact test following the 12J impact, both the permanent and maximum resistance changes surpassed those observed in samples exposed solely to the 20J impact test. This phenomenon can be ascribed to the fact that the same damaged area experienced a 20J impact after already undergoing a permanent resistance change due to the 12J impact energy level. Based on these results, it is evident that the impact damage of the material can be evaluated by analysing the resistance change, irrespective of whether it encounters damage at the same impact level repeatedly or different impact levels.

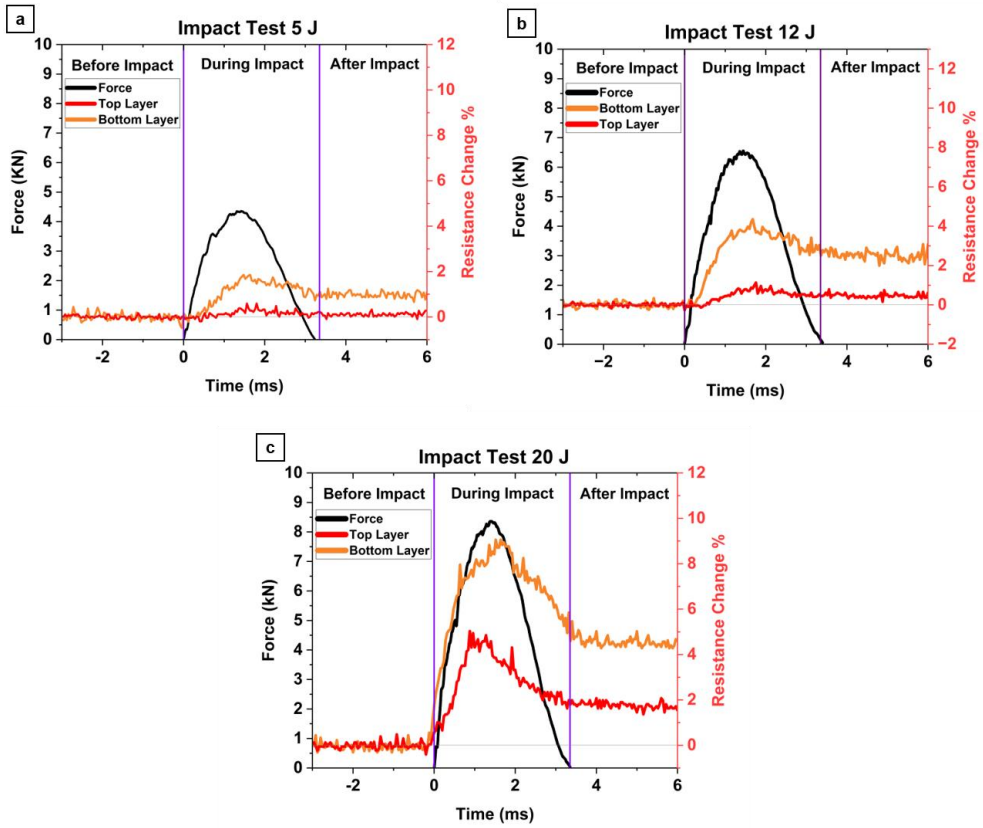

Figure 2. Resistance change results from top layer and bottom layer before, during and after impact test with impact force for different energy levels: a) 5J. b) 12J. c) 20J

Figure 5 presents the findings of the compression test conducted after the impact testing on GFRP and MWCNT-coated glass lamina embedded GFRP. The results indicate that the MWCNT-coated glass fibre did not have a significant impact on the residual strength. As anticipated, the residual strength of the specimens subjected to higher levels of impact energy noticeably decreased. The measured value after an impact energy of 20J demonstrated that the strength of the samples decreased by more than 50%. Based on these results, it is possible to estimate the remaining strength of the material by utilizing the resistance change measurements taken from two channels.

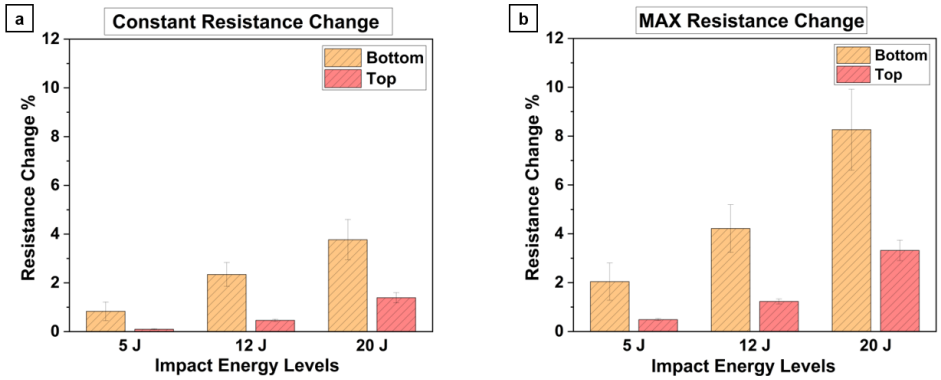

Figure 3. a) The constant resistance change of bottom and top layer after impact tests for different energy levels 5J,12J and 20J. b) The maximum resistance change during the impact test at different energy levels of 5J, 12J, and 20J for top and bottom layer of samples.

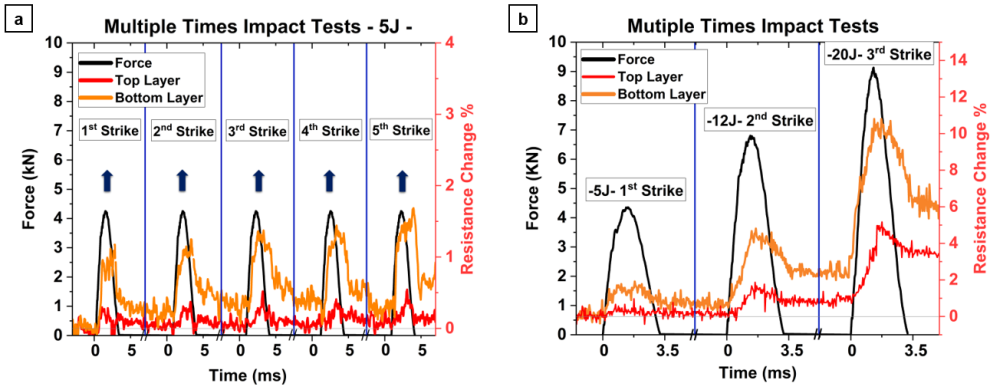

Figure 4. a) Resistance change from bottom and top layer of sample during a) 5 times impact test for 5J impact energy. b) 3 times impact test for 5J, 12J and 20J impact energy respectively.

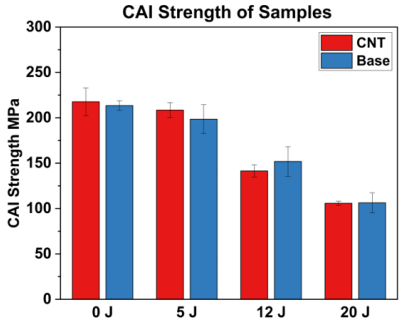

Figure 5. CAI strength of plain GFRP and MWCNT for different impacted energy levels.

CONCLUSION

This investigation focused on detecting BVID, a critical type of damage for composite materials. Unlike previous research, this study succeeded in detecting BVID through resistance values measured simultaneously from two different layers coated with MWCNT placed inside of the composite material. Additionally, a correlation was found between the resistance change and experiments conducted at various energy levels. Through the repeated impact test, the response of the system to multiple impacts was examined. Ultimately, this study demonstrated that the system could identify damage caused by different impact energy levels on the same material. Furthermore, compression tests were conducted on the samples after the impact test. The study revealed that this newly developed system not only detects BVID but can also predict the residual strength of the material.

REFERENCES

1. Diamanti K., Soutis C. Structural health monitoring techniques for aircraft composite structures. Progress in Aerospace Sciences. Elsevier; 2010; 46(8): 342–352. Available at: DOI:10.1016/j.paerosci.2010.05.001
2. Katnam KB., Da Silva LFM., Young TM. Bonded repair of composite aircraft structures: A review of scientific challenges and opportunities. Progress in Aerospace Sciences. 2013; 61: 26–42. Available at: DOI:10.1016/j.paerosci.2013.03.003
3. Güemes A., Fernandez-lopez A., Pozo AR. Structural Health Monitoring for Advanced Composite Structures : A Review. 2020; : 1–15.
4. Abdeljaber O., Avci O., Kiranyaz S., Gabbouj M., Inman DJ. Real-time vibration-based structural damage detection using one-dimensional convolutional neural networks. Journal of Sound and Vibration. Elsevier; 2017; 388: 154–170. Available at: DOI:10.1016/j.jsv.2016.10.043
5. McCrory JP., Al-Jumaili SK., Crivelli D., Pearson MR., Eaton MJ., Featherston CA., et al. Damage classification in carbon fibre composites using acoustic emission: A comparison of three techniques. Composites Part B: Engineering. Elsevier Ltd; 2015; 68: 424–430. Available at: DOI:10.1016/j.compositesb.2014.08.046
6. Viets C., Kaysser S., Schulte K. Damage mapping of GFRP via electrical resistance measurements using nanocomposite epoxy matrix systems. Composites Part B: Engineering. Elsevier Ltd; 2014; 65: 80–88. Available at: DOI:10.1016/j.compositesb.2013.09.049
7. Angelidis N., Wei CY., Irving PE. Response to discussion of paper: The electrical resistance response of continuous carbon fibre composite laminates to mechanical strain. Composites Part A: Applied Science and Manufacturing. 2006; 37(9): 1495–1499. Available at: DOI:10.1016/j.compositesa.2005.11.003
8. Dziendzikowski M., Kurnyta A., Dragan K., Klysz S., Leski A. In situ Barely Visible Impact Damage detection and localization for composite structures using surface mounted and embedded PZT transducers: A comparative study. Mechanical Systems and Signal Processing. Elsevier; 2016; 78: 91–106. Available at: DOI:10.1016/j.ymssp.2015.09.021
9. Polimeno U., Meo M., Almond DP., Angioni SL. Detecting low velocity impact damage in composite plate using nonlinear acoustic/ultrasound methods. Applied Composite Materials. 2010; 17(5): 481–488. Available at: DOI:10.1007/s10443-010-9168-5
10. Abrate S. Materials on Laminated Composite Lmpact. Most. 1991; 44(4).
11. Cawley P. Structural health monitoring : Closing the gap between research and industrial deployment. 2018; Available at: DOI:10.1177/1475921717750047
12. Kinloch IA., Suhr J., Lou J., Young RJ., Ajayan PM. Composites with carbon nanotubes and graphene: An outlook. Science. 2018; 362(6414): 547–553. Available at: DOI:10.1126/science.aat7439
13. Tugrul Seyhan A., Tanoglu M., Schulte K. Mode I and mode II fracture toughness of E-glass non-crimp fabric/carbon nanotube (CNT) modified polymer based composites. Engineering Fracture Mechanics. Elsevier Ltd; 2008; 75(18): 5151–5162. Available at: DOI:10.1016/j.engfracmech.2008.08.003